RESEARCH ARTICLE

An experimental investigation of rundown of the L-type calcium current [version 1; peer review: awaiting peer review]

Aditi Agrawal[1,2], Michael Clerx[1], Ken Wang[3], Evgenia Gissinger[3], David J. Gavaghan[2], Liudmila Polonchuk[3], Gary R. Mirams[1]

[1]School of Mathematical Sciences, University of Nottingham, Nottingham, England, NG7 2RD, UK
[2]Department of Computer Science, University of Oxford, Oxford, England, OX1 3QD, UK
[3]Pharma Research and Early Development, F. Hoffmann-La Roche, Innovation Center Basel, Switzerland

v1 **First published:** 14 May 2024, **9**:250
https://doi.org/10.12688/wellcomeopenres.20374.1
Latest published: 14 May 2024, **9**:250
https://doi.org/10.12688/wellcomeopenres.20374.1

Abstract

Background

L-type calcium channels (LCCs) are multi-protein macro-molecular ion channel complexes that are involved in several critical functions in cardiac, skeletal, neuronal, smooth muscle, and endocrine cells. Like other ion channels, LCCs can be selectively over-expressed in a host cell line and studied using voltage-clamp patch-clamp experiments. However, L-type calcium current (ICaL) recordings commonly exhibit a reduction in current magnitude over time, commonly termed 'rundown'. Previous studies have shown the effect of phosphorylation on rundown, here we provide evidence that accumulation of Ca^{2+} inside the cell also contributes towards ICaL rundown.

Methods

We generated experimental conditions that should promote the accumulation of sub-membrane Ca^{2+} in a CHO expression system, by increasing calcium import or decreasing export. These interventions took the form of: a decrease in inter-pulse duration between sweeps, block of the sodium-calcium exchanger, and increased temperature.

Results

On average, we found that current reduced to 63% of its initial value within 325 seconds. This reduction of current with time was found to follow two main patterns: linear or saturating decay. Additionally, current magnitude in some cells increased before stabilising or

Open Peer Review

Approval Status *AWAITING PEER REVIEW*

Any reports and responses or comments on the article can be found at the end of the article.

decaying.

Conclusions

This study shows that the rundown of ICaL in patch-clamp experiments can be reduced by modifying the experimental conditions, and implies that reduced accumulation of Ca^{2+} inside the cell membrane reduces calcium-dependent inactivation of ICaL.

Plain Language Summary

Cardiac electrical activity co-ordinates the heartbeat, and happens as a result of ion currents flowing in and out of cardiac muscle cells. One of these currents is known as the “Long-lasting” or “L-type calcium current” and is particularly prone to a phenomenon called “rundown” in which the magnitude of the current reduces over time in experimental recordings. It is often unclear whether this rundown represents real physiological processes or unwanted experimental limitations. In this article we vary experimental conditions to see which ones promote or reduce the amount of rundown using automated current recordings from cells that are made to express a lot of the proteins that form the channels which carry the current. The conditions that promote rundown are those in which we expect that the amount of calcium just under the cell membrane is highest. These conditions would be consistent with the idea that a lot of the rundown is due to a mechanism called calcium-dependent inactivation, a real physiological process, in which the L-type current reduces when there is a higher calcium concentration within the cell.

Keywords

calcium, rundown, L-type calcium channel, CaV1.2, calcium-dependent inactivation

Corresponding author: Gary R. Mirams (gary.mirams@nottingham.ac.uk)

Author roles: Agrawal A: Conceptualization, Data Curation, Formal Analysis, Investigation, Methodology, Software, Validation, Visualization, Writing – Original Draft Preparation, Writing – Review & Editing; **Clerx M**: Conceptualization, Formal Analysis, Methodology, Supervision, Writing – Review & Editing; **Wang K**: Conceptualization, Formal Analysis, Methodology, Supervision, Writing – Review & Editing; **Gissinger E**: Investigation; **Gavaghan DJ**: Conceptualization, Methodology, Project Administration, Supervision, Writing – Review & Editing; **Polonchuk L**: Conceptualization, Funding Acquisition, Methodology, Project Administration, Resources, Supervision, Writing – Review & Editing; **Mirams GR**: Conceptualization, Funding Acquisition, Methodology, Project Administration, Supervision, Writing – Original Draft Preparation, Writing – Review & Editing

Competing interests: K.W. & L.P. are employees of L.Hoffman-La Roche and K.W. is a shareholder. No other competing interests were disclosed.

Grant information: This work was supported by Wellcome [212203]; the UK Engineering and Physical Sciences Research Council [grant numbers EP/L016044/1, EP/S024093/1]; the Biotechnology and Biological Sciences Research Council [grant number BB/P010008/1]. A.A. acknowledges EPSRC and F. Hoffmann-La Roche Ltd. for studentship support via the Centre for Doctoral Training in Systems Approaches to Biomedical Science. D.J.G. acknowledges support from the EPSRC Centres for Doctoral Training Programme. G.R.M., M.C. and D.J.G. acknowledge support from a BBSRC project grant. G.R.M. and M.C. acknowledge support from the Wellcome Trust via a Wellcome Trust Senior Research Fellowship to G.R.M.
The funders had no role in study design, data collection and analysis, decision to publish, or preparation of the manuscript.

How to cite this article: Agrawal A, Clerx M, Wang K *et al.* **An experimental investigation of rundown of the L-type calcium current [version 1; peer review: awaiting peer review]** Wellcome Open Research 2024, **9**:250
https://doi.org/10.12688/wellcomeopenres.20374.1

First published: 14 May 2024, **9**:250 https://doi.org/10.12688/wellcomeopenres.20374.1

Introduction

The *L-type calcium channel* (LCC) is a multi-protein macro-molecular complex that conducts the L-type calcium current (I_{CaL}) and is found in neurons, cardiomyocytes, endocrine cells, and smooth muscle cells. In cardiomyocytes, the principal pore-forming α_1 subunit of LCCs is $Ca_V1.2$, encoded by the gene *CACNA1C*, while auxiliary units β and $\alpha_2\delta$ provide trafficking and regulatory functions[1]. Within the heart, I_{CaL} plays a key role of excitation-contraction coupling and maintenance of the plateau phase of the action potential. Unintended modulations of the LCC can lead to the development of long and short QT syndromes which expose a patient to the risk of sudden cardiac death. Brugada and Timothy syndromes are examples of such diseases that occur congenitally where LCCs are mutated[1].

The kinetics of ionic currents can be studied by performing patch-clamp experiments on cells overexpressing the channel(s) of interest. However, patch-clamp recordings of I_{CaL} are known to suffer from reduction of current magnitude over time, known as *rundown*. This effect is distinct from voltage-dependent ion channel gating, in that on repeated applications (*sweeps*) of the same voltage-clamp protocol, successive sweeps record smaller I_{CaL} magnitudes. Figure 1 shows an example of rundown of I_{CaL} recorded in whole-cell automated planar-patch voltage-clamp experiments on CHO cells overexpressing $Ca_V1.2$. The protocol used is shown in the figure's inset: membrane voltage (V_m) was repeatedly clamped at 0 mV for 150 ms interspersed by a *holding potential duration*, t_{hold}, of ten seconds at −90 mV.

Rundown in whole-cell patch-clamp experiments has been attributed to several factors including 'washing away' of phosphorylating agents (e.g. ATP) which would usually increase LCC activity[2] and loss of LCCs with time due to activation of Ca^{2+}-dependent enzymes that cause its proteolytic degradation[2,3]. Although modest rundown is reported for many ionic currents, it is exceptionally pronounced for the L- and N-type calcium currents[4]. Previous studies have found that use of buffers with a high chelating activity for calcium are associated with less rundown[2,3], suggesting that accumulation of Ca^{2+} inside the cell, near the membrane, could contribute to rundown. This hypothesis is further supported by the experimental observation of prominent rundown in ionic currents known to exhibit Ca^{2+}-dependent inactivation [e.g. I_{CaL}, 5]. In accordance with these literature findings, to reduce free Ca^{2+} in the cell, the intracellular solution in the experiment shown in Figure 1 included the calcium chelating buffer BAPTA. Similar experiments performed in the absence of any calcium chelating buffer result in almost no current being recorded.

In this study, we investigate the degree to which the accumulation of Ca^{2+} close to the intracellular side of the channel, and hypothesised subsequent calcium-dependent inactivation (CDI) of LCCs, can explain the observed I_{CaL} rundown. An automated patch-clamp machine was used to measure current from CHO cells overexpressing $Ca_V1.2$. Cells were subjected to variations in three factors of the experimental procedure:

- Temperature — at physiological temperatures I_{CaL} activates more fully than at room temperature which increases the current and therefore Ca^{2+} carried into the sub-membrane space; so we expect higher rundown at physiological temperatures.

- t_{hold} — the time between I_{CaL}-activating voltage clamp pulses. Larger gaps allow more time for free Ca^{2+} to: diffuse away from the submembrane space; react

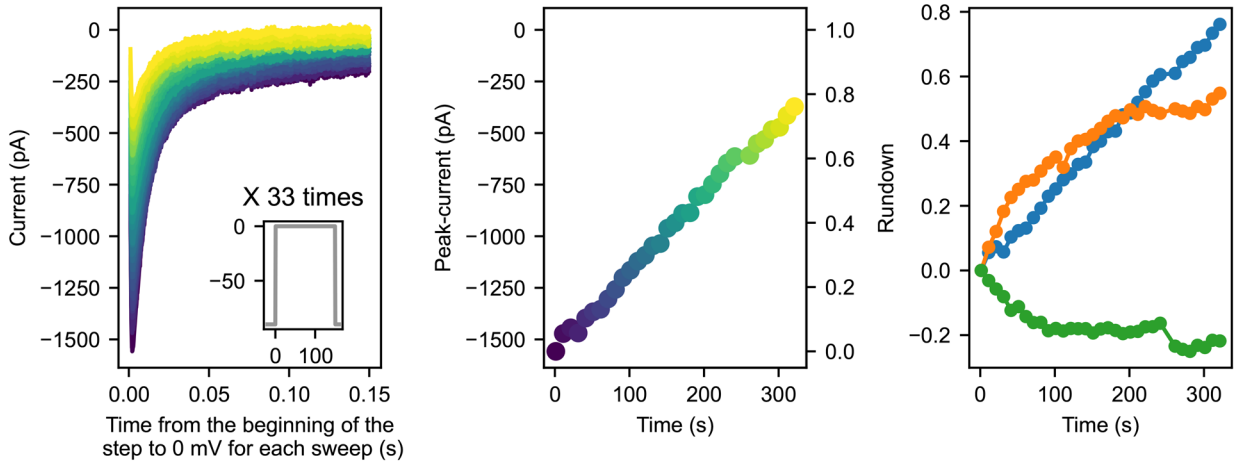

Figure 1. Rundown of the L-type calcium current. Left: I_{CaL} recorded at successive channel opening steps overlaid with first and last 150 ms step to 0 mV shown in indigo and yellow recordings respectively. An inset shows the voltage-clamp protocol during which current is recorded (in mV), it is interspersed by a potential of –90 mV held for t_{hold} = 10 s. Centre: peak I_{CaL} for each sweep shown on the left plot, represented on the right-hand axis as the proportion of current that has rundown. Right: examples of linear (blue), saturating (orange), and inverse (green) patterns of the rundown-versus-time plot.

with buffers (and/or for free buffer to diffuse towards the membrane); or be extruded by endogenous I_{NaCa}. Therefore, we expect higher rundown with shorter t_{hold}.

- I_{NaCa} block — pharmacological block of endogenous I_{NaCa} should result in reduced extrusion of Ca^{2+} and increase its concentration in the submembrane space; so we expect higher rundown in the presence of a pharmacological I_{NaCa} blocker.

Combinations of these conditions were explored in a full factorial design.

Increased rundown was observed for all experimental conditions expected to promote Ca^{2+} accumulation. This study thus provides experimental evidence that, at least in part, rundown can be explained by increased CDI or lack of recovery from CDI over the course of a patch-clamp experiment due to accumulation of Ca^{2+} in the submembrane space adjacent to LCCs.

Methods

This section describes the methods used in this study to record currents in a 384-well automated patch-clamp machine, post-process the recorded current to extract I_{CaL}, and select wells which met a set of quality control criteria. The design included three values for t_{hold} in the voltage-clamp protocol and two settings each for temperature and presence/absence of an I_{NaCa} blocker (3 × 2 × 2 = 12 conditions for a full factorial design). Wells were split into twelve groups with each group subjected to one of the twelve conditions.

Data processing was performed with Python version 3.9.5, Numpy version 1.21.5, and Pandas version 1.3.5. Multiple linear regression was run using the `'lm'` method in R version 4.3.1[6].

Voltage-clamp protocol

Three variations of the voltage-clamp protocol were used to set V_m. Each consisted of identical voltages, but varied in the time spent at holding potential between sweeps (t_{hold}, see below). A single 1.02 s sweep is shown in Figure 2 and consists of: a 10 ms step to −90 mV, a 100 ms step to −120 mV, a 400 ms ramp from −120 mV to −90 mV, a 350 ms step to −90 mV, a 150 ms step to 0 mV, and finally a 10 ms step to −90 mV. The step to −120 mV ensures that the LCCs are completely closed, while the ramp from −120 to −90 mV is used to calculate linear leak current (I_{leak}, see 'Post-processing'). Finally, the step to 0 mV ensures the maximum opening of the channel for the flow of I_{CaL}[7].

The three voltage-clamp protocols differ from each other in the inter-pulse duration t_{hold}, chosen to be 10 s, 20 s, or 40 s. All three inter-pulse durations are long enough for almost complete recovery from voltage-dependent inactivation and restoration to the steady state before each sweep. Therefore, when comparing any two sweeps in these protocols, voltage-dependent kinetics of I_{CaL} should remain the same, allowing observation of changes due solely to calcium-dependent kinetics or other experimental factors.

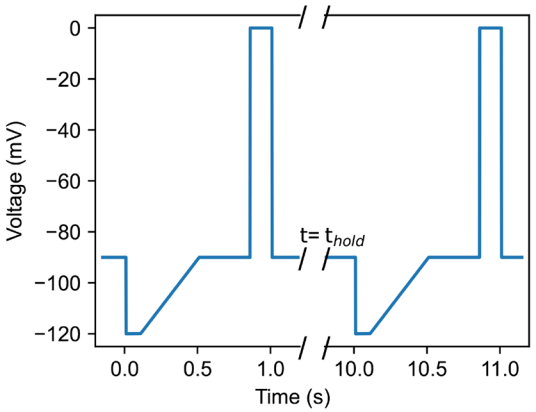

Figure 2. The voltage-clamp protocol used in the study, with the holding potential duration t_{hold} between successive sweeps set to either 10, 20, or 40 s.

Patch-clamp experiments

Whole-cell patch-clamp voltage-clamp experiments were performed using the SyncroPatch 384 patch engine (PE) platform serial number 39001160 (a Nanion Technologies GmbH product) with ready-to-use CHO cells[8] at passage 9[9], stably transfected[10] with $hCa_V1.2$ ($hCa_V1.2/\beta_2/\alpha_2\delta$-CHO stably transfected cell line, manufactured by ChanTest, catalogue number CT-CH004). This is a high-throughput automated patch-clamp system that allows simultaneous recordings from 384 wells (arranged into 16 rows and 24 columns) on a plate, each well contained a single, medium resistance hole (2.5–3.1MΩ). Cells in columns 1–12 were treated with 10 μM of the I_{NaCa} blocker ORM-10103 (25 mg from Sigma, catalogue number SML0972; causing >90% block[11]) while cells in columns 13–24 were treated with the control DMSO (100 mL of 0.1% strength from Sigma, catalogue number D2650). The experiment was performed at two temperatures: 298K and 310K, for each of the three voltage-clamp protocols equating to six chip plates (3 protocols × 2 temperature) and twelve experimental conditions (6 chip plates × 2 I_{NaCa} conditions) as shown in Figure 3.

Each well on the chip plate has a planar patch setup where the intracellular/pipette solution is attached to the cell interior via a *patch hole*, and this solution is expected to diffuse into a cell and dominate the concentrations in its cytosol[12]. Compositions of both 'bath' (extracellular) and intracellular solutions are given in Table 1. The intracellular solution was allowed to diffuse into the cell for 300 s before the voltage-clamp protocol was applied and current recordings began. At 325s, 10μM of the LCC blocker *nifedipine* (10g from Sigma, catalogue number N7634), which should selectively block I_{CaL} by at least 90%[13], was added and the experiment was run for a total of 561s. For t_{hold} values of 10s, 20s, and 40s, this duration equates to 33, 17, and 9 sweeps for each protocol before the addition of nifedipine, and 23, 11, and 5 sweeps after, respectively. At each sweep, current was recorded with a sampling frequency of 10kHz and machine estimates were taken of membrane capacitance (C_m), seal resistance (R_{seal}), and series resistance (R_s).

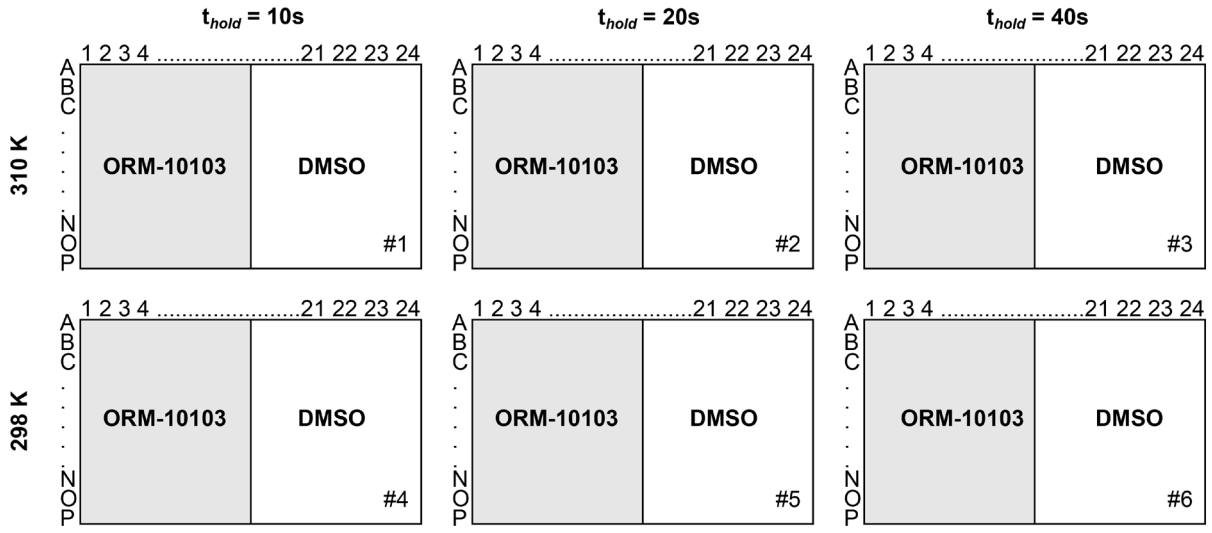

Figure 3. Chips used for patch-clamp experiments: Six 384-well automated patch clamp chips were used in this study, each corresponding to a unique combination of temperature and voltage-clamp protocol (t_{hold}). Half of each chip was also subject to block of I_{NaCa} with ORM-10103 (while the other half was on the control DMSO), resulting in 384 ÷ 2 = 192 wells per condition, and twelve conditions in total.

Table 1. Electrophysiology solutions for the $Ca_V1.2$ assay on the automated patch-clamp machine: the extracellular solution shows the resulting concentrations after sequential addition of half bath volume of "fill chip", "seal enhancer", and "reference" (twice) solutions. Each time the bath is full, the volume is halved so that the same volume of the next solution can be added, until there is a 1:1:6 proportion of the net extracellular solution. Therefore, the extracellular solution = 0.125×Fill chip + 0.125×Seal enhancer + (0.25 + 0.5)×Reference. The pH of the intracellular solution is 7.2, while that of the bath solutions varies from 7.2–7.4. The formula weight (F.W.) of each compound can be used to calculate the amount (g/L) in each solution.

Solution titrated with Osmolarity (mOsm) Compound	Supplier / Catalogue	F.W. g/mol	Intracellular *1M KOH* 260-300 mM	Fill chip *1M NaOH* 300-330 mM	Seal enhancer *1M HCL* 290-330 mM	Reference *1M HCL* 290-330 mM	Extracellular mM
KCl	Merck / K36782536	74.55	10	4	—	4	3.5
KF	Acros Organics / 201352500	58.09	100	—	—	—	—
NaCl	Merck / K38447104807	58.4	5	150	—	80	78.75
Na-ATP	Sigma / A2383	551	4	—	—	—	—
Na-GTP	Sigma / G8877	523.18	0.1	—	—	—	—
$CaCl_2$	Acros Organics / 349615000	110.99	—	1.2	10	1	2.15
$MgCl_2$	Merck / A914133908	203.3	—	1	1	1	1
CsCl	Fluka / 20966	168.36	—	—	4	—	0.5
BAPTA	Invitrogen / B1204	476.23	10	—	—	—	—
HEPES	Appllchem / A1069	238.3	10	10	10	10	10
Sorbitol	Sigma / S1876	182.17	—	—	—	40	30
N-Methyl-D-Glucamine	Fluka / 66930	195.21	—	—	130	40	46.25
D-(+) Glucose monohydrate	Fluka / 49149	198.17	—	5	5	5	5

Post-processing

Current measurements from the SyncroPatch were post-processed to reduce the effects of capacitive spikes, linear leak, and any background currents endogenous to the CHO cell. The method adopted to extract I_{CaL} from these recordings is described here.

Capacitive effect removal: When step-wise changes in the membrane voltage (V_m) occur, the recorded current is the sum of both capacitive and ionic current[14,15]. To remove any capacitive effects from the currents at each sweep i (I^i), recordings for 1 ms after the step-wise V_m changes (steps to −120, 0, and −90 mV in the voltage-clamp protocol, see inset plot in Figure 4C) were removed. The resulting currents are shown in Figure 4A–B for two sweeps.

Linear leak correction: The recorded current at each sweep i is contaminated by a linear leak current I^i_{leak} which occurs

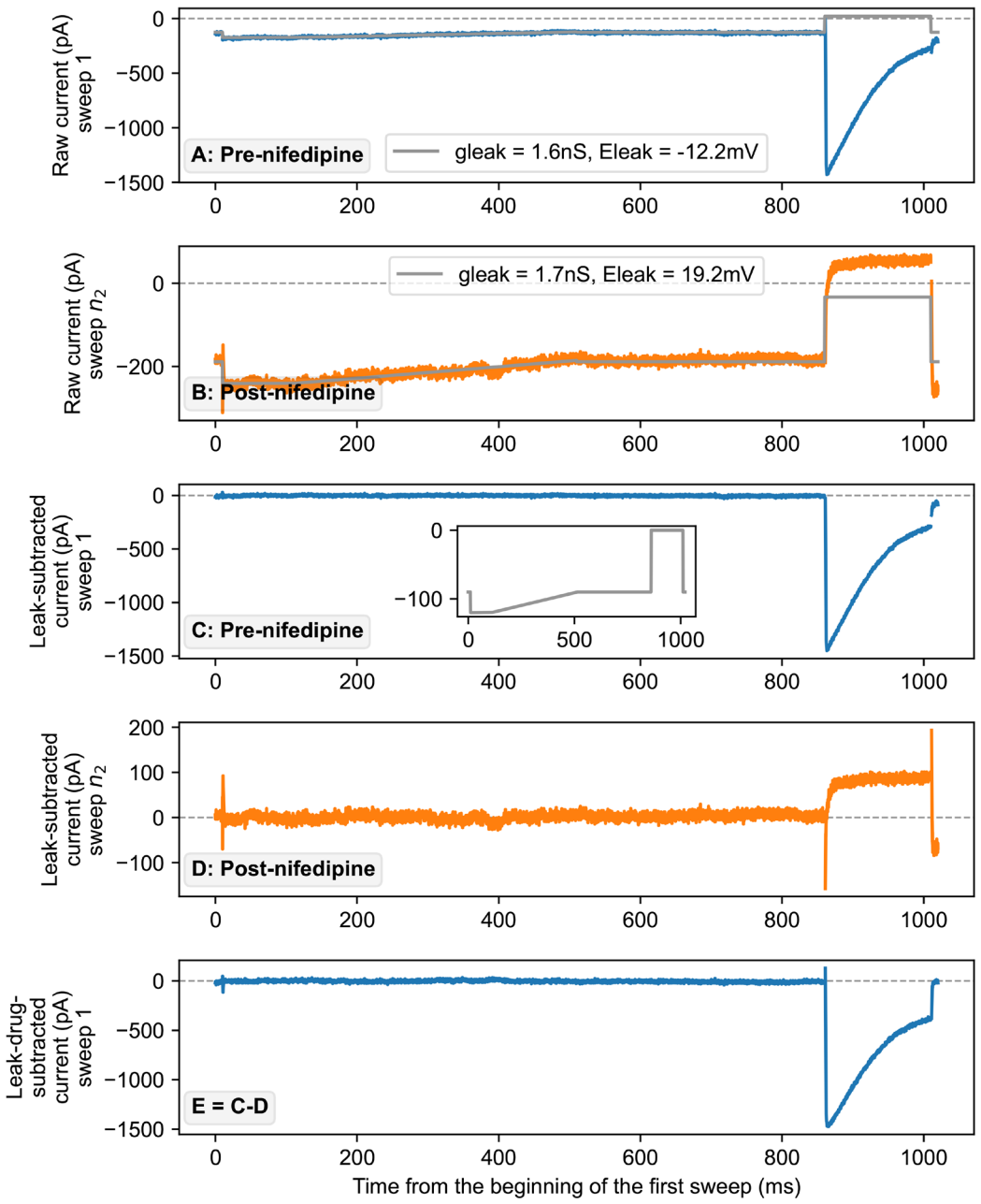

Figure 4. Illustration of the post-processing method used in this study: Current measured at sweep 1 (I^1) from cell in C19 of Chip 1 (see Figure 3). Panel **A** shows I^1 treated for capacitance, along with the linear leak current shown in grey. Panel **B** shows the current recorded in the second sweep after the application of I_{CaL} blocker (I^{n_2}) treated for capacitance, along with the linear leak current shown in grey. Panel **C** shows I^1 minus the fitted leak current, or $\hat{I}^1$. Panel **D** shows I^{n_2} minus the fitted leak current, or $\hat{I}^{n_2}$. Panel **E** shows I^1_{CaL}, which is the net I_{CaL} extracted from the sweep. Inset plot in Panel **C** shows the voltage-clamp protocol at each sweep, holding potential held at –90 mV, while the duration between steps to 0 mV is t_{hold}: 10 s, 20 s, or 40 s.

due to an imperfect R_{seal} (see Agrawal and Mirams[16] for details), given by:

$$I^i_{leak} = g^i_{leak}(V_m - E^i_{leak}), \quad (1)$$

here, g^i_{leak} and E^i_{leak} are the conductance and reversal potential of the leak current at sweep i. The parameters of I^i_{leak} were estimated by fitting the linear function in Equation 1 to I^i recorded during the voltage-ramp (−120 mV to −90 mV); a procedure similar to that used in Lei *et al.*[17]. These parameters were then used to calculate I^i_{leak} as a function of time (shown in grey in Figure 4A–B) and the resulting trace was subsequently subtracted from I_i to obtain leak subtracted current at each sweep i,

$$\hat{I}^i = I^i - I^i_{leak}, \quad (2)$$

where $\hat{I}^i$ is shown in Figure 4C–D for pre- and post-nifedipine recordings respectively.

Endogenous current correction: Finally, to isolate the current due to I_{CaL} at each sweep (I^i_{CaL}), non-I_{CaL} currents [e.g. endogenous current or non-linear leak, 18] were estimated and subtracted from every sweep. Non-I_{CaL} currents were identified as the current recorded after application of the LCC blocker *nifedipine*, therefore the second sweep after the addition of drug (n_2) was used to remove the effect of endogenous current:

$$I^i_{CaL} = \hat{I}^i - \hat{I}^{n_2}. \quad (3)$$

The use of this equation can be seen in Figure 4, where the plot in Figure 4D was subtracted from the plot in Figure 4C to obtain the plot in Figure 4E.

This process was applied to all sweeps recorded before the application of nifedipine, on all cells.

Quality control

Reliable recordings were identified by applying a series of quality control (QC) criteria to all wells. A preliminary QC0 was first applied to exclude recordings from wells in which the seal resistance did not remain measurable throughout the experiment. This resulted in the selection of only 74, 50, 52, 44, 56, and 40 cells out of 384 wells on the chip plates 1, 2, 3, 4, 5, and 6 respectively (Figure 3). The number of wells that remained for analysis was then reduced further using the following QC criteria:

1. QC1, Machine properties. QC1.1 excluded wells in which the R_{seal} was greater than 8GΩ or less than 0.1GΩ, QC1.2 excluded wells in which the recorded C_m was less than 1 pF (as this is probably not a CHO cell), and QC1.3 excluded wells in which the R_s was greater than 40MΩ as this leads to artefacts affecting the shape of the recorded ionic current.

2. QC2, Current contamination. QC2.1 excluded wells in which the magnitude of the peak current recorded during the channel opening step was less than the leak current (estimated using Equation 1), while QC2.2 excluded wells in which the magnitude of the endogenous current was greater than that of I_{CaL} (peak current during $\hat{I}^i < \hat{I}^{n_2}$).

3. QC3, Signal to noise. QC3 excluded wells with a signal-to-noise ratio below 50.

4. QC4, Variation in g_{leak}. QC4 excluded wells where R_{seal} deteriorated considerably through the experiment by removing those where the coefficient of variation of the calculated g_{leak} array from the first sweep to the one recorded up to two sweeps after the application of the LCC blocker (n_2), was greater than 2 (where g_{leak} was calculated from the −120mV to −90mV ramp shown in Figure 2).

5. QC5, Likelihood of being I_{CaL}. QC5 excluded recordings that were not likely to contain I_{CaL} by identifying wells in which there was a net influx of ions rather than outflow for more than 50% of sweeps of post-processed current (no reversal of current should be observed for I_{CaL} at 0mV).

The number of wells selected from each chip plate on the application of each QC criterion and the final number of wells selected after applying all QC criteria are given in Table 2.

Definitions

In the remainder of this manuscript, we adhere to the following two definitions.

Rundown at sweep i was denoted by R_i and quantified using peak I_{CaL} during the sweep's step to 0mV ($|I^i_{CaL}|_{max}$) relative to the same quantity in sweep 1: $R_i = 1 - |I^i_{CaL}|_{max} / |I^1_{CaL}|_{max}$ Figure 1 shows R_i for cell C19 of chip number 1 (Figure 3).

Rate of rundown at sweep i was denoted R'_i and calculated as: $R'_i = (R_{i+1} - R_i)/t_{hold}$, where t_{hold} was used in minutes. An overall rate of rundown for any cell, denoted R', was taken as the median R'_i of sweeps from 1 to $n - 1$, where n is the last sweep recorded before the application of the LCC blocker.

Results

Rundown

For cells that passed all QC criteria, the rundown for each sweep i (R_i, $i = 1 \ldots n$ where n is the last sweep recorded before the application of the LCC blocker), is shown in Figure 5. The results are shown in different subplots separated by the unique experimental conditions they were subjected to as part of the full factorial design which included changes in t_{hold}, temperature, and presence/absence of I_{NaCa} block.

Figure 5 shows that, irrespective of the differences in experimental conditions, a general trend of increase in rundown is observed as the experiment progresses. In extreme cases, rundown reduced the current to 14% of its initial value within 325 seconds. Qualitatively, three different shapes of

Table 2. Number of wells that passed each individual quality control (QC) criterion per chip: the last row shows the total number of wells selected on each chip, after all selection criteria have been applied. The QC criteria are explained in the text.

QC	310 K t_{hold} = 10*s*	310 K t_{hold} = 20*s*	310 K t_{hold} = 40*s*	298 K t_{hold} = 10*s*	298 K t_{hold} = 20*s*	298 K t_{hold} = 40*s*
QC0	74	50	52	44	56	40
QC1.1	63	44	37	43	55	37
QC1.2	74	50	50	44	56	40
QC1.3	74	48	48	44	55	36
QC2.1	65	43	43	39	55	40
QC2.2	46	37	26	31	43	36
QC3	48	34	31	19	40	32
QC4	73	47	50	44	55	38
QC5	70	45	49	42	56	40
All	36	24	18	18	35	25

rundown-versus-time curves are observed (Figure 1, right). The predominant pattern is a near-linear decrease with time (observed in 35% of cells), the second most common is saturation with time (observed in 22% of cells). The remaining cells (43%) have varying irregular shapes, where the most common shape has a 'reverse rundown' in which the current magnitude increases for the first few sweeps and saturates or decreases thereafter.

Effect of holding duration

In this section, the difference in R' across the varying voltage-clamp protocols (see 'Voltage-clamp protocol') is compared. The protocol with a smaller inter-pulse duration (t_{hold}) will allow the LCCs to open more frequently, allowing more Ca^{2+} to enter the cell. Therefore, if the intracellular [Ca^{2+}] contributes to rundown, then a decrease in rundown would be expected with an increase in t_{hold} (although, note that the amount of Ca^{2+} entering *per pulse via* I_{leak} will be roughly proportional to t_{hold}).

Figure 6 shows the distribution of observed rundown rate (R') in different experimental conditions, along with box plots indicating the median and interquartile range. Within each experimental condition, a slightly higher R' was observed for t_{hold} = 10 s, which decreased for 20 s, and then again for 40 s. Although this difference is small, we can observe a weak downward trend (we examine these trends using statistical methods below).

It is important to note that the primary difference in the incoming Ca^{2+} at the different t_{hold} is due to I_{CaL}, however, almost 44% of the Ca^{2+} could be brought into the cell by leak current (see 19), which could be interfering with the strength of the downward trend with increasing t_{hold}. Another factor possibly interfering with the trend could be an increase of R' caused e.g. by loss of phosphorylating agents and LCCs over time. Indeed, a plot comparing rundown per pulse across different experiments suggests that rundown also occurs due to time-dependent phenomena (see 19), as the rundown per pulse is largest for t_{hold} = 40 s (but is still smallest if considering rundown per minute). Nevertheless, the differences seen here suggest that the frequency at which Ca^{2+} enters the cell via L-type channels contributes to rundown rate, R'.

Effect of sodium-calcium exchanger block

Sodium-calcium exchangers are natively expressed in CHO cells and conduct I_{NaCa}, albeit at much lower levels than the artificially overexpressed I_{CaL}. I_{NaCa} removes Ca^{2+} from inside the cells in exchange for Na+[20,21]. If the accumulation of Ca^{2+} inside the cell contributes to rundown then more rundown would be expected for cells in which I_{NaCa} is blocked.

Figure 7 shows the R' distributions for all six combinations of experimental conditions (temperature and t_{hold}), separated such that I_{NaCa} is blocked on the left and not blocked on the right.

Across the six conditions, a slightly lower R' is observed when I_{NaCa} was not blocked. Similar to the previous sub-section, this difference is small. Nevertheless, the increase in R' on the application of an I_{NaCa}-blocker suggests that the accumulation of Ca^{2+} inside the cell contributes to rundown. It is important to note that while the blocker ORM-10103 is highly selective for I_{NaCa}[11], it has also been known to alter the I_{CaL} kinetics at the concentrations used in this study[11], thereby possibly interfering with the current recordings.

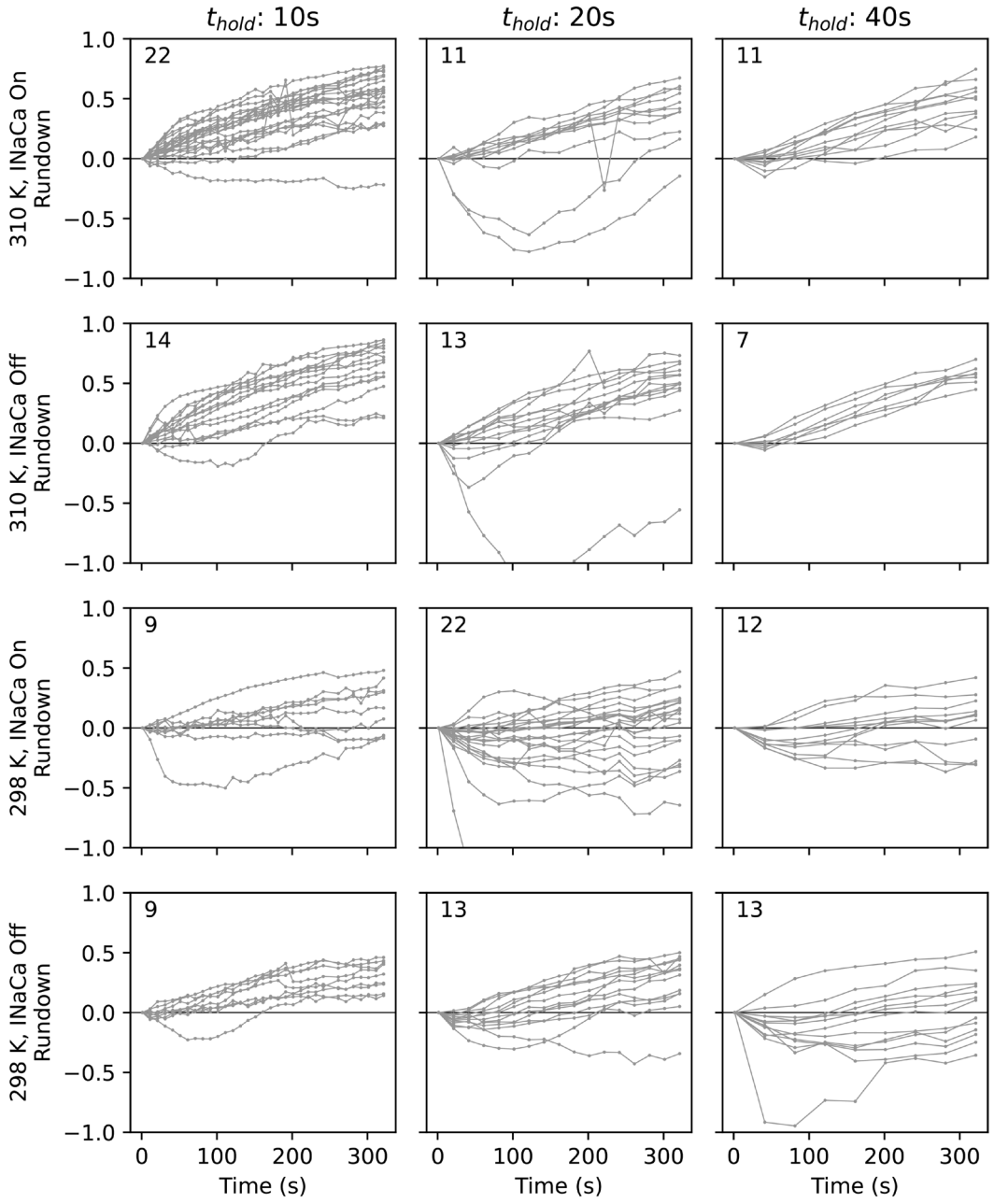

Figure 5. Rundown at different experimental conditions: The rundown recorded for all cells passing quality control, for each of the twelve experimental conditions. The number of cells in each subplot is given in the upper left corner. Note: a missing data point in the first column at approximately 250 s is due to output bandwith limitations of the patch-clamp machine.

Effect of temperature

Experiments were performed at 310 K and 298 K. The magnitude of I_{CaL} is known to be lower at room temperature than at physiological temperature[22], and so the Ca^{2+} influx is also lower at room temperature. As a result, more rundown is expected at a higher temperature. The increase in temperature should also accelerate I_{NaCa}, but this effect should be negligible due to the much higher expression levels of LCCs.

Figure 8 shows that for all 6 combinations of experimental conditions of t_{hold} and I_{NaCa} block, R' is noticeably more pronounced at the higher temperature.

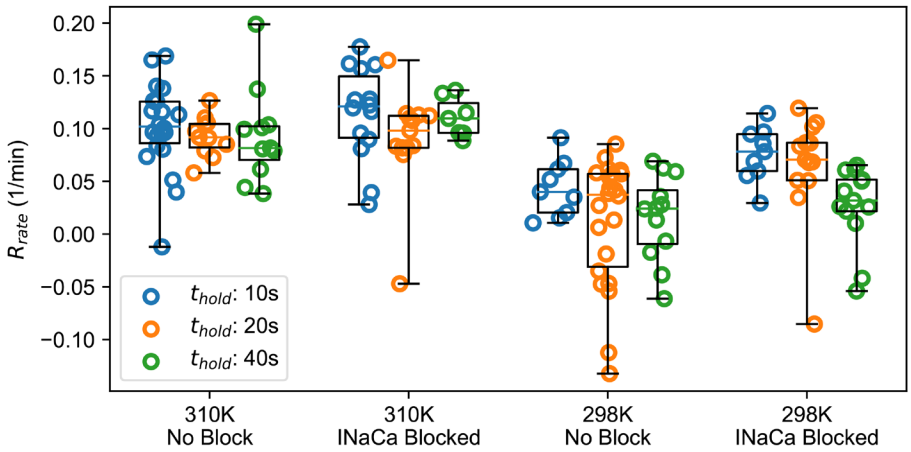

Figure 6. Change in rundown rate (*R′*) due to holding potential duration (t_{hold}): The different experimental conditions are segregated on the x-axis. Within each experimental condition, the *R′* can be compared across cells with a t_{hold} of 10 s, 20 s, and 40 s. The box-plot shows the interquartile range along with the median rate at each condition. The whiskers show the range of the data points.

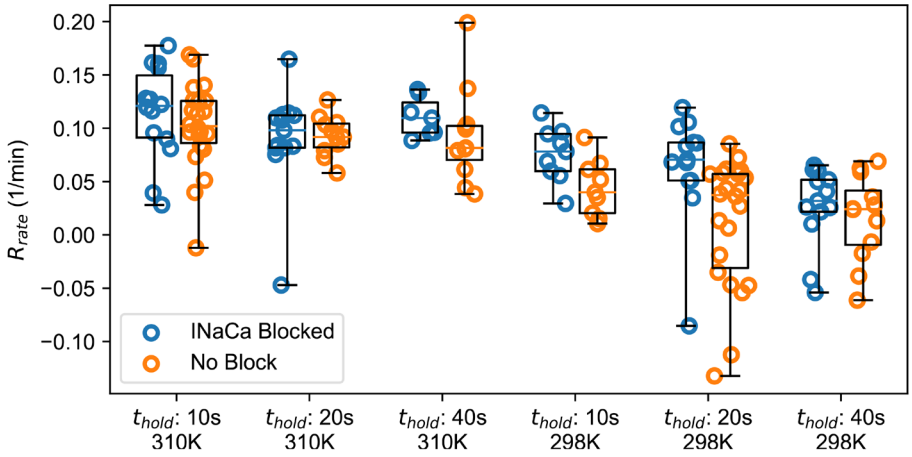

Figure 7. Change in rundown rate (*R′*) due to I_{NaCa}: The different experimental conditions are segregated on the x-axis. Within each experimental condition, the *R′* can be compared across cells where I_{NaCa} was blocked and where it was not. The box-plot shows the interquartile range along with the median rate at each condition. The whiskers show the range of the data points.

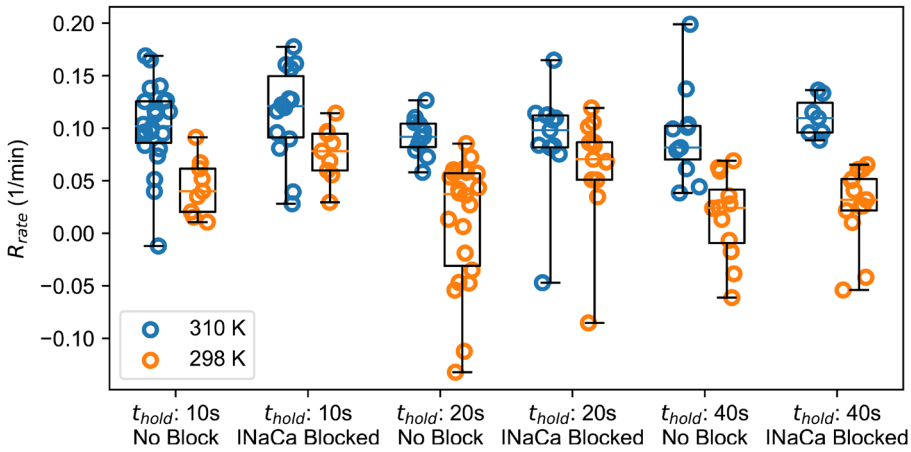

Figure 8. Change in rundown rate (*R′*) due to temperature: The different experimental conditions are segregated on the x-axis. Within each experimental condition, the *R′* can be compared across cells where temperature varies from 310 K to 298 K. The box-plot shows the interquartile range along with the median rate at each condition. The whiskers show the range of the data points.

Although CHO cells do not have an endoplasmic reticulum (SR), they are known to have other internal reservoirs of Ca^{2+} which may release Ca^{2+} into the cell at higher temperature[23,24], further increasing CDI-induced rundown.

Combined effect of all experimental conditions

Multiple linear regression analysis was used to examine how R' was influenced by the independent experimental conditions of t_{hold}, presence/absence of I_{NaCa}, and temperature. The linear regression took the form

$$R' = \beta_0 + \beta_1 \log(t_{hold}) + \beta_2(\mathbb{1}_{NaCa}) + \beta_3(\mathbb{1}_{298K}) + \epsilon, \qquad (4)$$

where ϵ is noise for each cell, encapsulating factors not included in the regression, and is assumed to be drawn from a Normal distribution, $N(0, \sigma^2)$. Here '$\mathbb{1}$' denotes an indicator function, that is $\mathbb{1}_{NaCa} = 0$ when I_{NaCa} is blocked and 1 otherwise, and $\mathbb{1}_{298K} = 0$ at 310K and 1 at 298K. We systematically explored the addition of each experimental factor, revealing statistically significant improvement in the model fit ($p < 0.05$) with each inclusion. The final model, incorporating all three conditions, demonstrated a substantial reduction in the residuals and was highly significant ($F(3, 152) = 34.42$, $p < 2.2 \times 10^{-16}$). The adjusted coefficient of determination ($R2 = 0.39$) indicated that the experimental conditions explained approximately 39% of the variance in R' across the cells.

Moreover, as we had hypothesised that all three coefficients should be non-zero and negative (see 'Introduction') one-sided t-test yielded $p < 0.05$ for all coefficients with $\beta_1 = -0.016$ ($p = 0.00671$), $\beta_2 = -0.021$ ($p = 0.00161$), and $\beta_3 = -0.062$ ($p = 2.08 \times 10^{-15}$), see Figure 9. This result reinforces the conclusion that R' decreases when: t_{hold} increases; I_{NaCa} is not blocked; and temperature is decreased, both individually and in combination. Thus the result supports our hypothesis that calcium-dependent inactivation explains some of the rundown, and confirms that the rundown rate trends shown in Figure 6, Figure 7, and Figure 8 are significant. Tests of the regression assumptions and exact p-values can be viewed in the extended analysis[19].

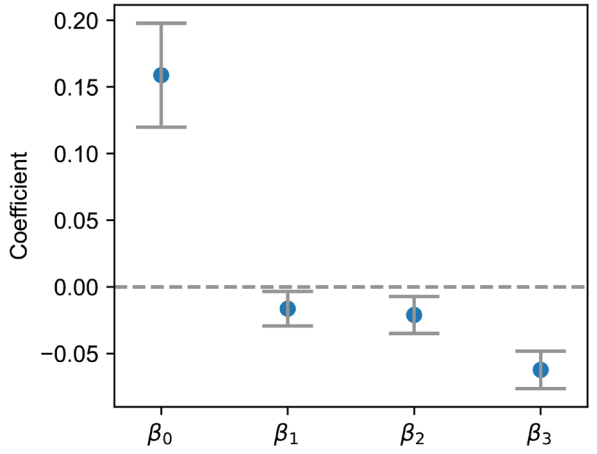

Figure 9. β coefficients obtained from the multiple linear regression of Equation (4) to the complete dataset, and their 95% confidence intervals (shown in grey). β_0 is the baseline rundown rate. In terms of factors that vary between our experiments, β_1 is the coefficient associated with the length of the experiments, β_2 is associated with presence of I_{NaCa}, β_3 is associated with lower temperature, and all of these factors lower the rundown rate.

Discussion

L-type calcium channels (LCCs) are known to inactivate not just in response to voltage, but also to calcium[1]. Experimental recordings of I_{CaL} suffer from more rundown than most other ion channels[4]. We investigated whether calcium-dependent inactivation (CDI) of LCCs contributes to rundown of I_{CaL}. This was done by measuring the rate of rundown (R') of I_{CaL} from cells subjected to experimental conditions purposefully designed to either increase or decrease accumulation of intracellular sub-membrane Ca^{2+}. Since the patch-clamp experiment was run on all cells for the same time duration, the rundown from other known factors such as washing away of phosphorylating agents and loss of LCCs[2–4,25] can be assumed to be similar across all cells so that this experimental setup allows us to study rundown due to CDI.

The current was found to deteriorate at an average rate of 8% of its initial magnitude per minute. Three shapes of the rundown-versus-time curve were recorded across the cells. The most common shape was an almost linear rundown of I_{CaL} with time, followed by a saturating shape in which the level of rundown stabilises with time. Rundown was found to be higher at conditions in which there is hypothesised to be an increased accumulation of $[Ca^{2+}]$ inside the cell. This was evident from the higher rate of rundown (R') at increased temperature, block of I_{NaCa}, and decrease in t_{hold}.

There was substantial variability observed in the R' across different cells across all experimental conditions. Nearly 40% of the variability in the rate of rundown (R') across cells could be explained by the experimental factors we varied, but 60% could not. Some cells also showed 'irregular' rundown, where the peak I_{CaL} that was recorded increased for the first few sweeps followed by a decrease in current magnitude. The differences in these irregular shapes could not be explained by only the changes in t_{hold}, temperature, or presence/absence of an I_{NaCa} blocker.

The available buffer beneath the cell membrane is expected to be strongly influenced by cell size and the time between a cell being patched and the experimental recording beginning. It is possible that the extent of diffusion of free buffer into the cell affects the observed shape of the rundown-versus-time curve, with CDI present at the beginning of the experiment being removed as buffer diffuses in, causing increased peak currents and explaining more of the well-well variability in rundown patterns. Another factor that will influence the submembrane accumulation of Ca^{2+} is LCC expression level. In future work, we are undertaking a

modelling analysis of these processes to systematically investigate their potential implications for the CDI-dependent rundown of I_{CaL}.

Previous work has shown that rundown is pronounced for cardiac LCCs observed in the whole-cell configuration[2,4]. The use of ATP reduces rundown of I_{CaL}, therefore we used compounds that included ATP in the intracellular solution of our experimental setup (see Table 1)[2,26]. Similarly, because the use of Ca^{2+}-chelating buffers reduces rundown[2], we used a 'fast' buffer (BAPTA) in our intracellular solution. Despite performing the patch-clamp experiments in a whole-cell configuration, in the presence of ATP and BAPTA, fast rundown was still observed. Our study confirms that this can be partially explained by the accumulation of Ca^{2+} in the submembrane, and quantifies its contribution.

Practically, our results suggest that larger intervals between current activation pulses and room temperature conditions should minimise I_{CaL} rundown.

Conclusions

Rundown of I_{CaL} in whole-cell patch-clamp experiments was found to be fast, with an average deterioration rate of 8% per minute. Qualitatively, the current was found to attenuate with time in three different patterns: linearly decaying, saturating decay, and 'irregular' patterns where current increased transiently before saturating or decaying.

This study strongly suggests that I_{CaL} rundown is partly explained by calcium dependent inactivation, as in the full factorial design experiment a higher rundown was observed in experimental conditions that would promote the accumulation of Ca^{2+} inside the cell membrane. These experimental factors of temperature, inter-pulse duration, and presence/absence of sodium-calcium exchanger block were able to explain approximately 40% of the variability in rundown rate across wells.

Data availability

All data, code, and supporting material are available at https://github.com/CardiacModelling/L-type-Ca-rundown-experiments, including additional supporting plots[19]. A permanently archived version is available on Zenodo[16].

Acknowledgements

The authors thank Michael A. Colman (University of Leeds) and Denis Noble (University of Oxford) for their feedback based on careful reading of an earlier draft of this work as part of A.A.'s Doctorate of Philosophy thesis.

References

1. Hofmann F, Flockerzi V, Kahl S, *et al.*: **L-type $Ca_v1.2$ calcium channels: from in vitro findings to in vivo function.** *Physiol Rev.* 2014; **94**(1): 303–326.
PubMed Abstract | Publisher Full Text

2. Belles B, Malécot CO, Hescheler J, *et al.*: **"Run-down" of the Ca current during long whole-cell recordings in guinea pig heart cells: role of phosphorylation and intracellular calcium.** *Pflugers Arch.* 1988; **411**(4): 353–360.
PubMed Abstract | Publisher Full Text

3. Sarantopoulos C, McCallum JB, Kwok WM, *et al.*: **β-escin diminishes voltage-gated calcium current rundown in perforated patch-clamp recordings from rat primary afferent neurons.** *J Neurosci Methods.* 2004; **139**(1): 61–68.
PubMed Abstract | Publisher Full Text

4. Kameyama M, Kameyama A, Kaibara M, *et al.*: **Intracellular mechanisms involved in "run-down" of calcium channels.** In: *Calcium Protein Signaling.* Springer, 1989; 111–117.
Publisher Full Text

5. McNaughton NC, Bleakman D, Randall AD: **Electrophysiological characterisation of the human N-type Ca^{2+} channel II: activation and inactivation by physiological patterns of activity.** *Neuropharmacology.* 1998; **37**(1): 67–81.
PubMed Abstract | Publisher Full Text

6. R Core Team: **R: a language and environment for statistical computing**. R Foundation for Statistical Computing, Vienna, Austria, 2020.
Reference Source

7. Agrawal A, Wang K, Polonchuk L, *et al.*: **Models of the cardiac L-type calcium current: a quantitative review.** *WIREs Mech Dis.* 2023; **15**(1): e1581.
PubMed Abstract | Publisher Full Text | Free Full Text

8. Gazzano-Santoro H, Chan LG, Ballard MS, *et al.*: **Ready-to-use cryopreserved primary cells: a novel solution for QC lot release potency assays.** *Bioprocess Int.* 2014; **12**(2): 28–39.
Reference Source

9. Mather JP, Roberts PE: **Introduction to cell and tissue culture: theory and technique**. Springer Science & Business Media, 1998.
Publisher Full Text

10. Fus-Kujawa A, Prus P, Bajdak-Rusinek K, *et al.*: **An overview of methods and tools for transfection of eukaryotic cells *in vitro*.** *Front Bioeng Biotechnol.* 2021; **9**: 701031.
PubMed Abstract | Publisher Full Text | Free Full Text

11. Jost N, Nagy N, Corici C, *et al.*: **ORM-10103, a novel specific inhibitor of the Na^+/Ca^{2+} exchanger, decreases early and delayed afterdepolarizations in the canine heart.** *Br J Pharmacol.* 2013; **170**(4): 768–778.
PubMed Abstract | Publisher Full Text | Free Full Text

12. Milligan CJ, Möller C: **Automated planar patch-clamp.** *Methods Mol Biol.* 2013; **998**: 171–187.
PubMed Abstract | Publisher Full Text

13. Shen JB, Jiang B, Pappano AJ: **Comparison of L-type calcium channel blockade by nifedipine and/or cadmium in guinea pig ventricular myocytes.** *J Pharmacol Exp Ther.* 2000; **294**(2): 562–570.
PubMed Abstract

14. Armstrong CM, Bezanilla F: **Charge movement associated with the opening and closing of the activation gates of the Na channels.** *J Gen Physiol.* 1974; **63**(5): 533–552.
PubMed Abstract | Publisher Full Text | Free Full Text

15. Hille B: **Ion channels of excitable membranes.** Sinauer Associates, Inc., Sunderland, Massachusetts, 2001.

16. Agrawal A, Mirams G: **CardiacModelling/L-type-Ca-rundown-experiments: v1.01.** 2024.
http://www.doi.org/10.5281/zenodo.10044849

17. Lei CL, Clerx M, Gavaghan DJ, *et al.*: **Rapid characterization of hERG channel kinetics I: using an automated high-throughput system.** *Biophys J.* 2019; **117**(12): 2438–2454.
PubMed Abstract | Publisher Full Text | Free Full Text

18. Lei CL, Fabbri A, Whittaker DG, *et al.*: **A nonlinear and time-dependent leak current in the presence of calcium fluoride patch-clamp seal enhancer [version 2; peer review: 4 approved].** *Wellcome Open Res.* 2021; **5**: 152.
PubMed Abstract | Publisher Full Text | Free Full Text

19. Agrawal A, Mirams G: **Github: Extended data supporting the study of rundown experiments on L-type calcium current.** 2024.
https://github.com/CardiacModelling/L-type-Ca-rundown-experiments/blob/main/ExtendedData.ipynb

20. Blaustein MP, Lederer WJ: **Sodium/calcium exchange: its physiological implications.** *Physiol Rev.* 1999; **79**(3): 763–854.
PubMed Abstract | Publisher Full Text

21. Ottolia M, Torres N, Bridge JHB, *et al.*: **Na/Ca exchange and contraction of the heart.** *J Mol Cell Cardiol.* 2013; **61**: 28–33.
PubMed Abstract | Publisher Full Text | Free Full Text

22. Wang R, Karpinski E, Pang PKT: **Temperature dependence of L-type calcium channel currents in isolated smooth muscle cells from the rat tail artery.** *J Therm Biol.* 1991; **16**(2): 83–87.
Publisher Full Text

23. Iredale PA, Hill SJ: **Increases in intracellular calcium via activation of an endogenous P2-purinoceptor in cultured CHO-K1 cells.** *Br J Pharmacol.* 1993; **110**(4): 1305–10.
PubMed Abstract | Publisher Full Text | Free Full Text

24. Gamper N, Stockand JD, Shapiro MS: **The use of Chinese Hamster Ovary (CHO) cells in the study of ion channels.** *J Pharmacol Toxicol Methods.* 2005; **51**(3): 177–185.
PubMed Abstract | Publisher Full Text

25. Ono K, Fozzard HA: **Phosphorylation restores activity of L-type calcium channels after rundown in inside-out patches from rabbit cardiac cells.** *J Physiol.* 1992; **454**(1): 673–688.
PubMed Abstract | Publisher Full Text | Free Full Text

26. Weiss S, Shimrit O, Benmocha A, *et al.*: **Regulation of cardiac L-type Ca^{2+} channel $Ca_v1.2$ via the β-adrenergic-cAMP-protein kinase A pathway: old dogmas, advances, and new uncertainties.** *Circ Res.* 2013; **113**(5): 617–631.
PubMed Abstract | Publisher Full Text